

Comb-on-Plane Switching Electrodes for Liquid Crystal Displays

Zhiguo Meng, Hoi S. Kwok and Man Wong*

Department of Electrical and Electronic Engineering
The Hong Kong University of Science and Technology
Clear Water Bay, Kowloon
Hong Kong

Abstract

Though the common twisted-nematic (TN) liquid crystal displays have excellent contrast and low color dispersion, they suffer from small viewing angle when driven into the homeotropic state. Among the many techniques proposed, "in-plane-switching" (IPS) has been quite effective in improving the viewing angles. However, there may be difficulty in adopting the conventional IPS to higher definition displays because it suffers from limited storage capacitance and reduced transmittance. A new comb-on-plane switching (COPS) electrode design is presently proposed. Compared to the conventional IPS, COPS allows for lower switching voltage and offers advantages including naturally scalable storage capacitance, wide viewing angle with TN-like high transmittance and low color dispersion.

Keywords: liquid crystal displays, electrodes, viewing angle.

* Corresponding author: Tel. +852 2358 7057, Fax. +852 2358 1485, Email: eemwong@ee.ust.hk

Introduction

Compared to the displays based on the venerable cathode ray tubes (CRTs), liquid crystal displays (LCDs) offer some unique advantages including lower power consumption and increased portability resulting from their smaller form factors and lighter weight for equivalent display areas. It is no wonder that LCDs have not only dominated the portable display market but also made significant in-roads into markets traditionally held by CRTs [1].

Twisted-nematic (TN) liquid crystals (LCs) are commonly employed in active matrix (AM) LCDs because they offer low drive voltage, true white and dark states [2], as well as ease of implementing gray scale and color displays. The principal drawback of the common TN LCDs is their narrow viewing angle, which limits their use in applications requiring wide viewing angles, such as television sets, end graphic monitors, digital museums or libraries, etc. A number of techniques have been proposed to increase the viewing angles of the common TN LCDs, such as the use of retardation films in the front and in the back of the LC cells. However, such displays are difficult to optimize and the material cost as well as the added steps in manufacturing are undesirable.

Recognizing that the narrow viewing angles are associated with the homeotropic state in the common TN LCDs, Oh-e *et al.* [3] and Ohta *et al.* [4] eliminated such a state by using in-plane switching (IPS) of the LC molecules to produce wide viewing angles without film compensation [1,5]. However, while IPS has been rather effective in increasing the viewing angle, it suffers from low transmittance [6] and requires an electrode configuration that limits storage capacitance.

Several improvements have been suggested to overcome the drawbacks of the original implementation of the IPS scheme. Lee *et al.* [7] proposed the use of top and bottom grid electrodes to introduce a "4-domain" switching structure. Shin *et al.* [8] proposed the use of common electrodes on the opposite sides of an LC cell to enhance the transmission. Kim *et al.*

[9] proposed the use of non-straight electrodes so that there was a “2-domain”-like structure [10] upon switching. Lee *et al.* [6,11] proposed the use of closely spaced electrodes to realize “fringing field” switching of negative LC.

A new comb-on-plane switching (COPS) electrode design is presently proposed. While some of the liquid crystal molecules are switched in the plane of the display, the electrode arrangements and the principle of its operation are different from those of the conventional IPS. Consequently, COPS allows for faster switching at a lower switching voltage and offers advantages including naturally scalable storage capacitance, wide viewing angle with TN-like high transmittance and low color dispersion, much easier electrode fabrication than those of IPS, and amenable to large scale production.

COPS Structure and Cell Fabrication

The proposed COPS electrode configuration (Fig. 1) consists of a comb electrode on top of an insulated plane electrode. 60nm sputtered indium tin oxide (ITO) and 200nm low temperature oxide (LTO) were used to form the electrodes and the inter-electrode insulation, respectively. For the top comb electrode, the width (W_c) of and the separation (W_s) between the fingers were made the same in the present implementation. $W_c = W_s$ values of 2, 3, 4 and 5 μ m have been investigated.

When a potential difference, V_c , is applied across the comb and the plane electrodes, the desired switching electric field, $\vec{E}(x, y)$, is established, emanating from the comb fingers and terminating on the exposed plane electrode in between the fingers. The magnitude of $\vec{E}(x, y)$ decays rapidly in the direction normal to the plane of the COPS electrodes. An estimation of $\vec{E}(x, y)$ distribution above the comb electrode is shown in Figure 2.

Furthermore, where the fingers overlap the plane electrode, scalable storage capacitors (C_s) are naturally obtained, as indicated in Figure 1a.

A schematic of the completed LC cell is shown in Figure 3. The cell gap was $12\mu\text{m}$ and TN0403 positive LC, with a birefringence (δn) of 0.258, was used. The COPS electrodes were placed on the bottom glass plate. The rubbed polyimide (PI7121) layer aligned the LC molecules parallel to the long axes of the comb fingers while the polarizer was aligned perpendicularly. For the top glass plate, no electrodes were placed and both the rubbing of the polyimide layer and the polarizer were aligned perpendicularly to the long axes of the comb fingers on the bottom glass plate.

For comparison, conventional IPS TN0403-LC cells with cell gaps of $5\mu\text{m}$ and ITO electrode spacing of $9\mu\text{m}$ were also fabricated. The rubbing of the polyimide layers on the top and the bottom glass plates were parallel to the long axes of the ITO electrodes so that the LC molecules were homogeneously aligned. Crossed polarizers were used and the cells were opaque when no voltage was applied.

The cell gaps for the COPS and the IPS cells were different because the two switching modes required different optimization strategies.

COPS Electric Field Estimation

Ignoring the LTO induced gap between the comb and the plane electrodes, one can approximate the electrode configuration as shown in Figure 2a. The electrical potential $V(x, y)$ above the comb electrode is governed by Laplace' Equation:

$$\nabla^2 V = 0.$$

Using separation of variables and applying the symmetry condition $V(x, y) = V(-x, y)$, the periodic condition $V(x + W_s + W_c, y) = V(x, y)$ and the boundary conditions:

$$V(x,0) = \begin{cases} 0, & 0 < x < \frac{W_s}{2} \\ V_c, & \frac{W_s}{2} < x < \frac{W_s + W_c}{2} \end{cases},$$

one can show that

$$V(x,y) = -V_c \sum_{n=1}^{\infty} \frac{2}{n\pi} \left(\sin \frac{\kappa n}{2} \pi \cos n \frac{x}{W} \pi \right) e^{-n \frac{y}{W} \pi},$$

where $2W \equiv W_s + W_c$ and $0 < \kappa \equiv \frac{W_s}{W} \leq 1$. $\vec{E}(x,y)$ can then be deduced:

$$E_x = -\frac{\partial V}{\partial x} = -\frac{V_c}{2W} \left[\frac{e^{\frac{y}{W}\pi} - \cos\left(\frac{\kappa}{2} - \frac{x}{W}\right)\pi}{\cosh \frac{y}{W}\pi - \cos\left(\frac{\kappa}{2} - \frac{x}{W}\right)\pi} - \frac{e^{\frac{y}{W}\pi} - \cos\left(\frac{\kappa}{2} + \frac{x}{W}\right)\pi}{\cosh \frac{y}{W}\pi - \cos\left(\frac{\kappa}{2} + \frac{x}{W}\right)\pi} \right],$$

$$E_y = -\frac{\partial V}{\partial y} = -\frac{V_c}{2W} \left[\frac{\sin\left(\frac{\kappa}{2} - \frac{x}{W}\right)\pi}{\cosh \frac{y}{W}\pi - \cos\left(\frac{\kappa}{2} - \frac{x}{W}\right)\pi} + \frac{\sin\pi\left(\frac{\kappa}{2} + \frac{x}{W}\right)\pi}{\cosh \frac{y}{W}\pi - \cos\left(\frac{\kappa}{2} + \frac{x}{W}\right)\pi} \right],$$

where E_x and E_y are the horizontal and vertical components of $\vec{E}(x,y)$, respectively. For

the present implementation, $W_c = W_s = W \Rightarrow \kappa = 1$, one obtains:

$$E_x = -2 \frac{V_c}{W} \frac{\sin \frac{x}{W} \pi \cosh \frac{y}{W} \pi}{\cos 2 \frac{x}{W} \pi + \cosh 2 \frac{y}{W} \pi},$$

$$E_y = -2 \frac{V_c}{W} \frac{\cos \frac{x}{W} \pi \cosh \frac{\pi}{W} y}{\cos 2 \frac{x}{W} \pi + \cosh 2 \frac{y}{W} \pi}.$$

The electric field distribution has been shown in Figure 2b. For large y , the following

approximations for E_x and E_y apply:

$$E_x \approx -2 \frac{V_c}{W} \left(\sin \frac{x}{W} \pi \right) e^{-\frac{y}{W} \pi},$$

$$E_y \approx -2 \frac{V_c}{W} \left(\cos \frac{x}{W} \pi \right) e^{-\frac{y}{W} \pi}.$$

Therefore, as y is increased, $\overset{w}{E}(x, y)$ decays exponentially. The characteristic decay length can be controlled by selecting a suitable W for the comb electrodes. For an LC cell gap larger than a few multiples of W , only the alignment of the LC molecules close to, but not those far away from, the COPS electrodes are directly affected by $\overset{w}{E}(x, y)$. The creation of this fast decaying, "surface" electric field is a unique and important feature of the COPS electrode design.

Experimental Results

The transmittance-voltage curve (TVC) of the COPS cell is compared to those of the common TN and the conventional IPS cells in Figure 4. The transmittance of the COPS cell increases monotonically with increasing V_c and eventually saturates at high V_c . This is unlike the case of the conventional IPS cells employing voltage switching of the LC molecules from the homogenous to the twisted state, the transmittance decreases with increasing driving voltage after peaking at a certain intermediate voltage.

The select voltage, defined as the V_c required to achieve 90% of the maximum transmittance, is plotted as a function of W in Figure 5. A linear dependence is obtained, agreeing with the analytical results showing the magnitude of $\overset{w}{E}(x, y)$ being proportional to V_c/W . Consequently, low voltage operation and pixel size scaling could be realized by reducing W without sacrificing the electric field strength.

The switching characteristics of the COPS and the IPS cells are shown in Figures 6 and 7, respectively. For the same TN0403 LC and with V_c switching between 0 and 5V, respective rise and fall times of 10ms and 20ms were obtained for the COPS cell. For the IPS

cell, the rise time ($\propto 1/E^2$) was a longer 50ms because of the reduced electric field strength resulting from the larger electrode separation.

The dispersion spectra of the COPS and the TN cells are compared in Figure 8. It can be concluded that the dispersion characteristics of the COPS cell are very similar to those of the common TN cell.

The viewing angle of the COPS cell has been measured using an Autronic DMS501 measurement system. The angular distributions of the relative transmittance and the contrast ratio (CR) at $V_c = 5V$ are shown in Figures 9 and 10, respectively. A maximum CR of 90 and $CR > 20$ for all viewing angles are obtained. The transmission reduces as the viewing angle deviates from the normal, but 70% relative transmission is obtained for viewing angle up to 45° in all directions.

The characteristics of the COPS, the common TN and the conventional IPS cells are summarized and compared in Table I. It can be concluded that a host of favorable characteristics makes COPS highly applicable to realizing high definition and highly transmissive AMLCDs with wide viewing angles.

Discussions

The presently proposed COPS configuration is equivalent to the conventional IPS configuration at the limit of zero spacing between the alternating powered and grounded electrodes. The problem of electrical shorting between two co-planar inter-digitated electrodes with zero separation is eliminated in the COPS design by the insulated comb and plane electrodes. Both W_s and W_c of the comb electrode are determined by one masking level and no relative alignment is required between the comb and the plane electrodes.

Common electrode frame inversion is believed to be the best driving scheme for high definition AMLCDs, especially for polysilicon thin film transistor addressed pixel matrices.

Since storage capacitor over gate gives rise to voltage instability during frame inversion, it is best if the capacitor is formed between the common and the pixel electrodes. This can be accomplished effortlessly using the COPS electrode design, where scalable capacitors are obtained at the naturally occurring overlap region - approaching 50% of the pixel area in the present implementation - between the comb finger and the plane electrodes. On the contrary, valuable pixel areas must be set aside in conventional IPS cells to implement the required capacitors, leading to significantly reduced aperture ratio and further reducing the brightness of IPS cells relative to that of the COPS cells.

90°-TN cells with parallel polarizers were fabricated and the resulting COPS cells were dark when $V_c = 0V$. When $V_c \neq 0V$, the LC molecules are re-aligned by the resulting electric field, as shown in Figure 11. Near the edges (Locations E) of the fingers, the electric field is largely horizontal ($E_y = 0$) and perpendicular to the long axes of the fingers. The LC molecules immediately above the electrodes are re-aligned accordingly. The twist of the LC molecules relative to that of the LC molecules near the top glass plate is reduced and the overall alignment of the LC molecules approaches the homogeneous state. Near the centers (Locations C) of the fingers and the gaps, the electric field is largely vertical ($E_x = 0$) and the tilt of the LC molecules immediately above the electrodes is increased, resulting in a reduction of the birefringence. In the regions between Locations E and C, the twist and the tilt of the LC molecules immediately above the electrodes are, respectively, reduced by the horizontal and increased by the vertical components of the electric field. In all cases, the amount of the twist, hence also the rotation of the polarization, is reduced and the cell becomes transparent. The degree of reduction depends on the magnitude of V_c and gray scale can be obtained.

To understand the similarity between excellent transmission and color dispersion characteristics of the COPS and the TN cells, one can evaluate the general expression for the transmission coefficient (T) of a TN cell sandwiched between two parallel polarizers [2]:

$$T = \left(\cos \Phi \cos \beta d + \frac{\Phi}{\beta d} \sin \Phi \sin \beta d \right)^2 + \left(\frac{\Delta k}{\beta} \right)^2 \sin^2 \Phi \sin^2 \beta d,$$

in which

$$\Delta k \equiv \frac{\pi \Delta n}{\lambda} \quad \text{and} \quad \beta^2 \equiv \left(\frac{\Phi}{d} \right)^2 + \Delta k^2,$$

where Φ , Δn , d and λ , are the total twist angle, the birefringence, the cell gap and the optical wavelength, respectively.

For a TN cell, $\Delta n = 0$ and $\Phi = \pi/2$ when selected. T approaches 100% and is independent of λ , hence non-dispersive. For a COPS cell, particularly near the edges of the comb fingers, $\Phi = 0$ when selected, $T \approx \cos^2 \beta d + \sin^2 \beta d = 1$, which is also almost 100% and independent of λ .

More insight into the switching of the COPS cell can be gained by studying the LC Parameter Space (PS) [2] shown in Figure 12. The starting state of a COPS cell is marked by Point D, which represents a 90° TN state and the display is dark. When V_c is applied and increased, the LC molecules near Location C in Figure 11 are re-aligned by the vertical electric field. The resulting tilt angle changes from near 0° to near 90° and Δn reduces from 0.25 toward 0. This state is marked by Point T in the PS. The LC molecules near Location E in Figure 11 are re-aligned by the horizontal electric field. Φ decreases from 90° to near 0°, the tilt angle and Δn are unchanged. This is marked by Point G in the PS. In between Locations E and C, the selected states of the LC molecules are represented by the line joining Points T and G, with both reduced Φ and Δn . Consequently, many quasi-TN modes are

present, each with its distribution of viewing angles. The display is transmissive and wide viewing angle is obtained.

Conclusions

In the work, highly transmissive and wide viewing angle LC cells based on COPS electrode design is proposed. Compared to the conventional IPS cells, the COPS cells allow for lower switching voltage and offer advantages including TN-like high transmittance and low color dispersion. Scalable storage capacitors can be obtained as a natural consequence of the electrode design.

References

1. S. Kaneko *et al*, Wide Viewing Angle and High Definition TFT-LCD Technologies, Proceedings of the 18th International Display Research Conference (Asia Display'98), pp. 33, 1998.
2. H. S. Kwok, Parameter Space Representation of Liquid Crystal Display Operating Modes, Journal of Applied Physics, pp. 3687-3693, 80(7), October. 1996.
3. M. Oh-e *et al*, Principle and Characteristics of Electro-Optic Behavior with In-Plane Switching Mode, Proceedings of the 15th International Display Research Conference (Asia Display'95), pp. 577-580, 1995.
4. M. Ohta *et al*, Development of Super TFT LCDs with In-Plane Switching Display Mode, Proceedings of the 15th International Display Research Conference (Asia Display'95), pp. 707-710, 1995.
5. K. Kondo, Materials and Components Optimization for IPS TFT-LCDs. Proceedings of SID'98, pp. 389, 1998.
6. S. H. Lee *et al*, High Transmittance, Wide Viewing Angle Nematic Liquid Crystal Display Controlled by Fringing Field Switching, Proceedings of the 18th International Display Research Conference (Asia Display'98), pp. 371, 1998.
7. S. H. Lee *et al*, Multi-domain-like Homeotropic Nematic LCD, SID Symposium Digest, pp. 702-705, 1998.
8. H. H. Shin *et al*, Hybrid Switching Mode for Wide Viewing Angle TFT LCD, SID Symposium Digest, pp. 718-721, 1998.
9. K. H. Kim *et al*, New LCD Modes for Wide Viewing Angle Applications, SID Symposium Digest, pp. 1085-1088, 1998.
10. A. Takeda *et al*, A Super High Image Quality Multi-Domain Vertical Alignment LCD by New Rubbingless Technology. SID Symposium Digest, pp.1077, 1998.

11. S. H. Lee *et al*, A Novel Wide-Viewing Angle Technology: Ultra-Trans View. SID Symposium Digest, pp.202-205, 1999.

List of Tables:

Table I. Comparison of performance parameters of the common TN, the conventional IPS and the COPS cells.

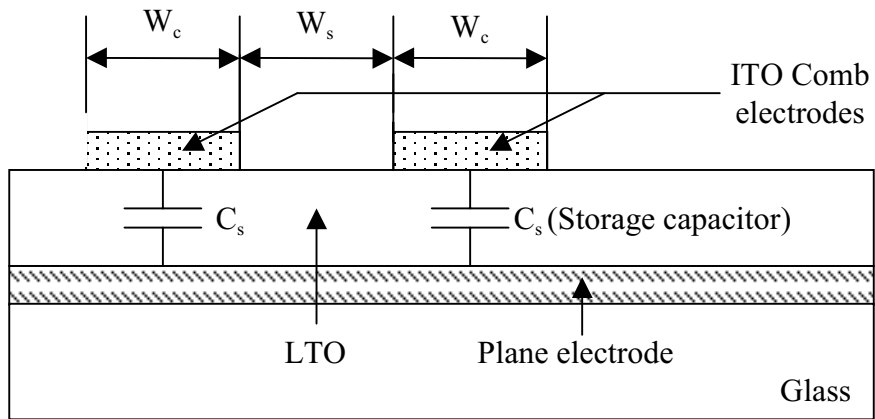
List of Figures:

- Figure 1: Schematic cross-section (a) and plan-view (b) diagrams of the comb-on-plane switching (COPS) electrode design. C_s is the storage capacitance.
- Figure 2: Approximate electric field distribution above the comb electrode.
- Figure 3: Schematic diagram of the completed COPS LC cell showing the LC molecules in the twisted state.
- Figure 4: Comparison of the transmittance-voltage curves (TVC) of the COPS ($W = 3 \mu\text{m}$, $d = 12 \mu\text{m}$), the common TN ($d = 5 \mu\text{m}$) and the conventional IPS ($W = 9 \mu\text{m}$, $d = 5 \mu\text{m}$) cells.
- Figure 5: Dependence of the select voltage on the comb finger width (and spacing) of the COPS cell.
- Figure 6: Switching characteristics of the COPS cell.
- Figure 7: Switching characteristics of the conventional IPS cell.
- Figure 8: Experimental relative dispersion spectra of the common TN and the COPS cells.
- Figure 9: Angular distribution of the relative light intensity (RI) of the COPS cell in the bright state.
- Figure 10: Angular distribution of the contrast ratio (CR) of the COPS cell.
- Figure 11: Schematic diagram of the COPS cell in the selected state. The LC molecules are re-aligned by the electrical field.
- Figure 12: Parameter Space (PS) diagram showing the transitions of the COPS cell.

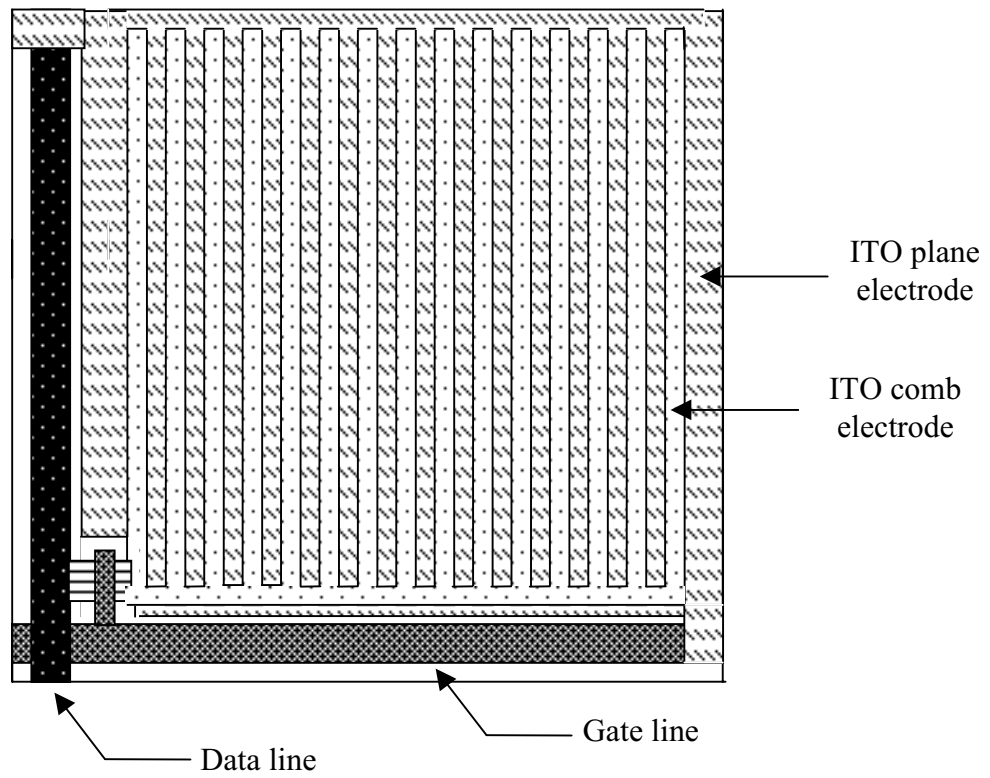
Table I.

	TN cell	IPS cell	COPS cell
Viewing angle (Relative intensity > 70%)	40-60° (White mode)	90~110°	80~120°
Maximum transmission relative to the TN cell	100%	67%	95%
Maximum measured contrast ratio	200	200	90
Rise time (ms)	N/A	50	10
Storage capacitance in pixel	Large	Very small	Large

Figure 1.



(a)



(a)

Figure 2.

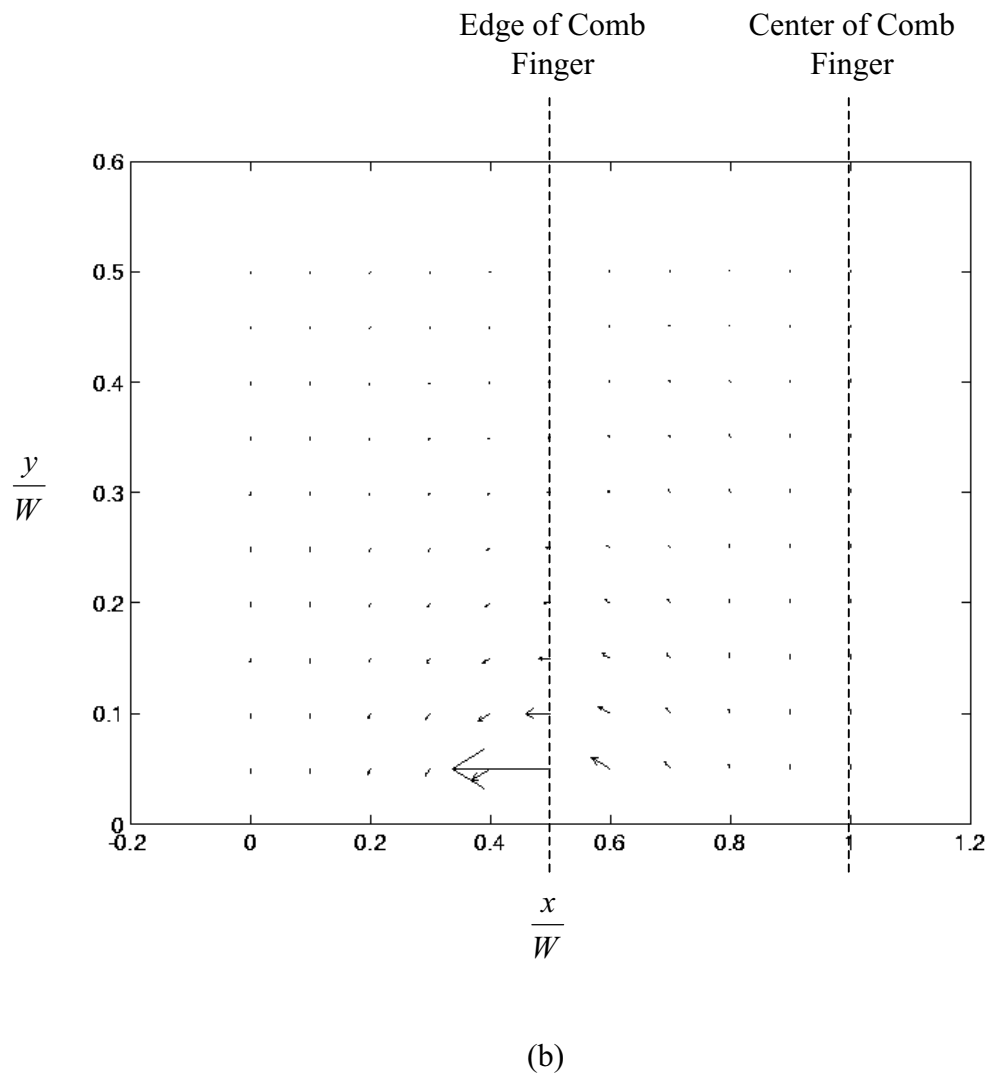
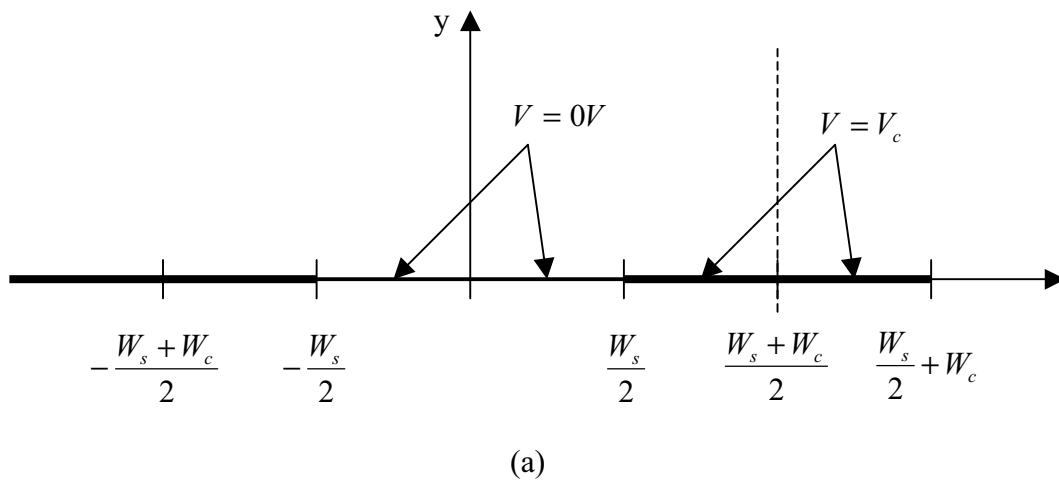


Figure 3.

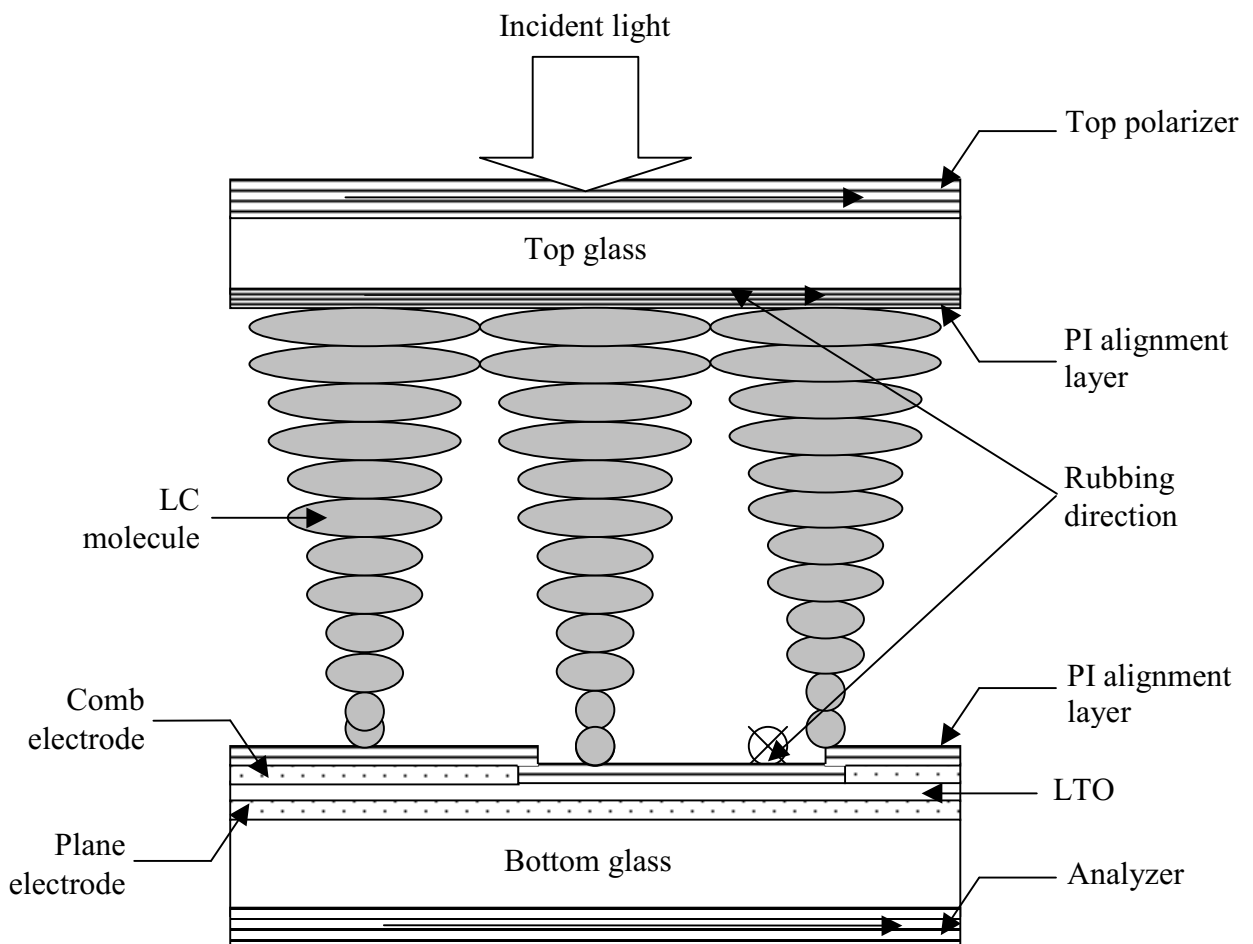


Figure 4.

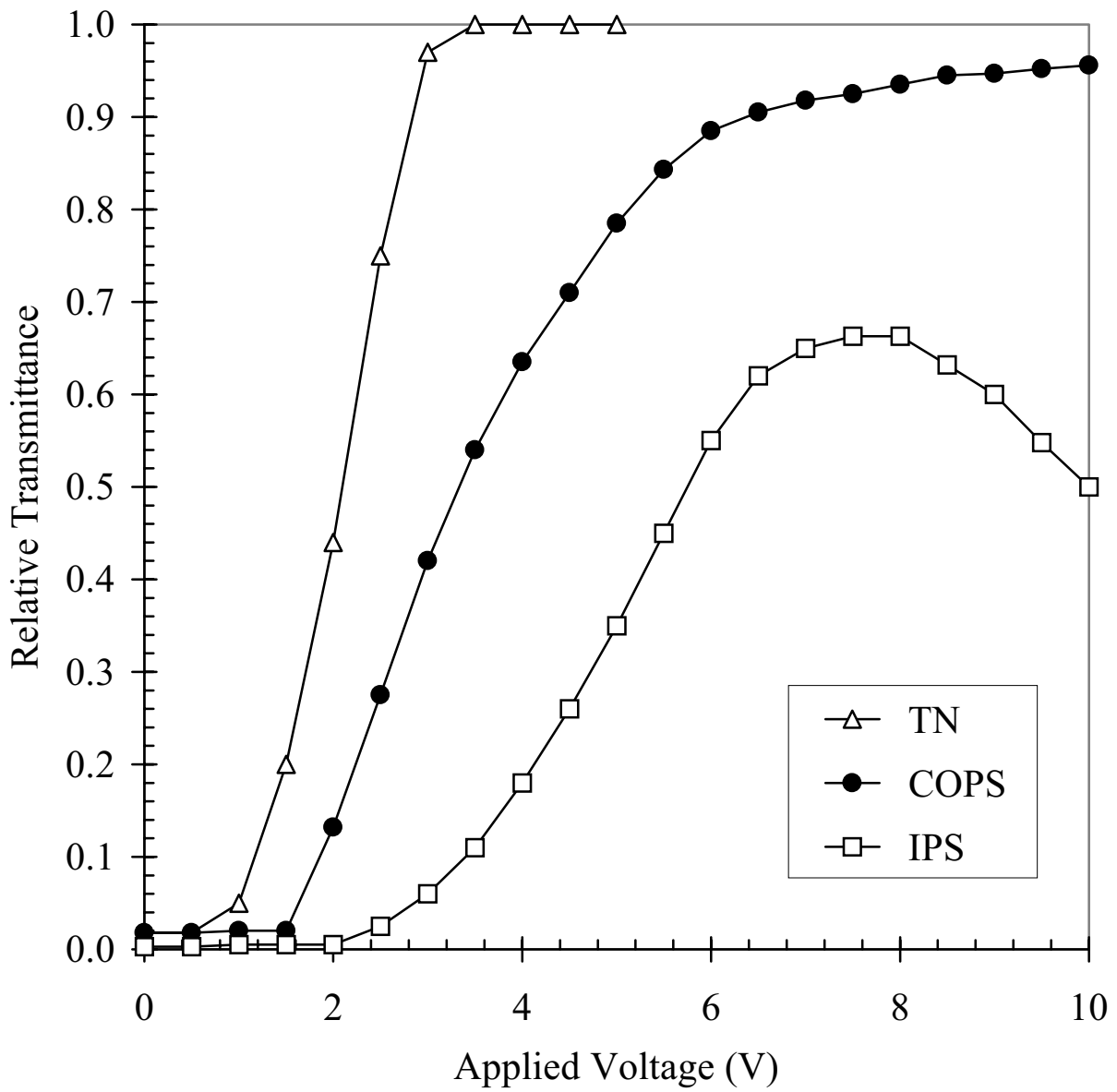


Figure 5.

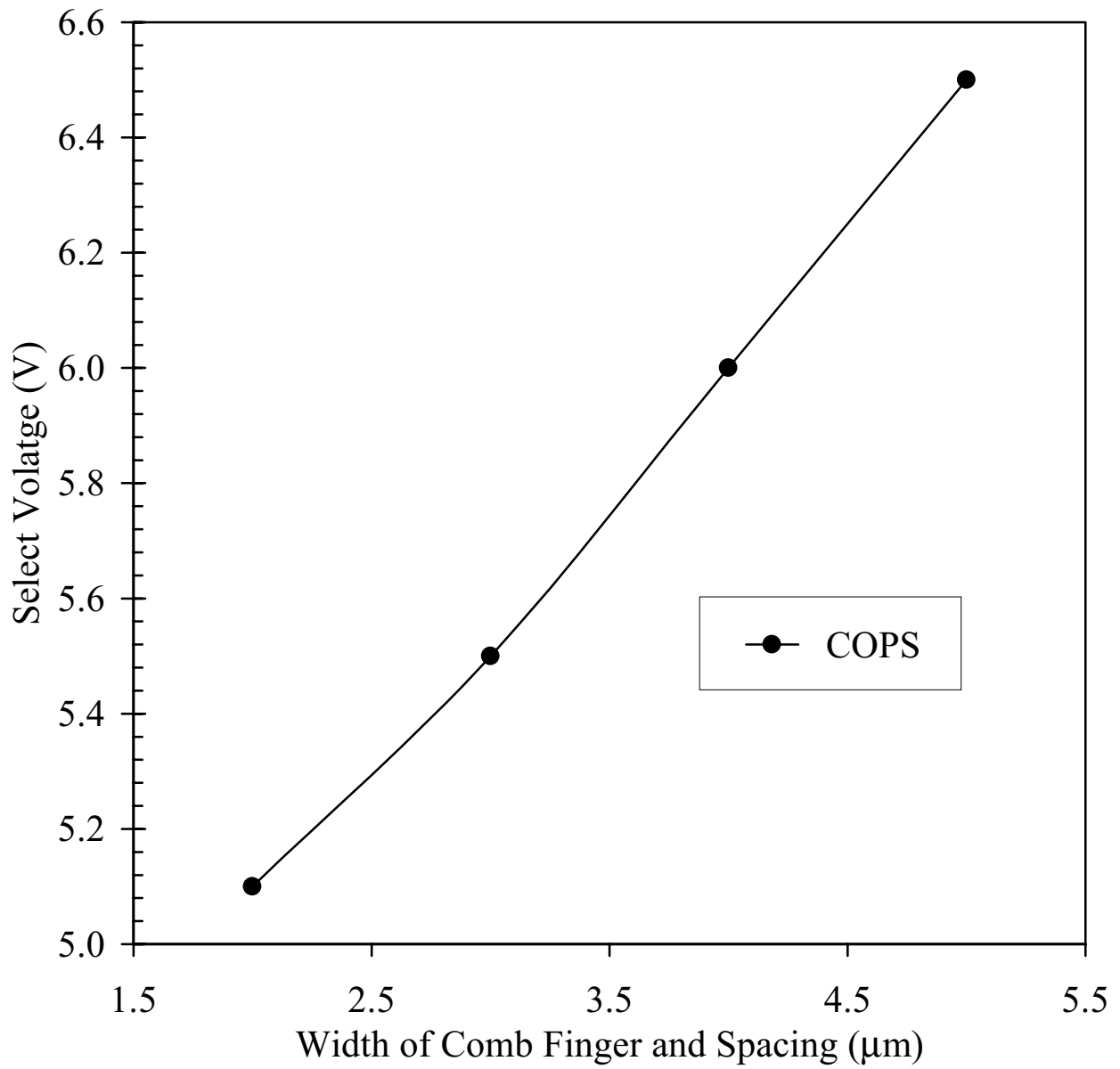


Figure 6.

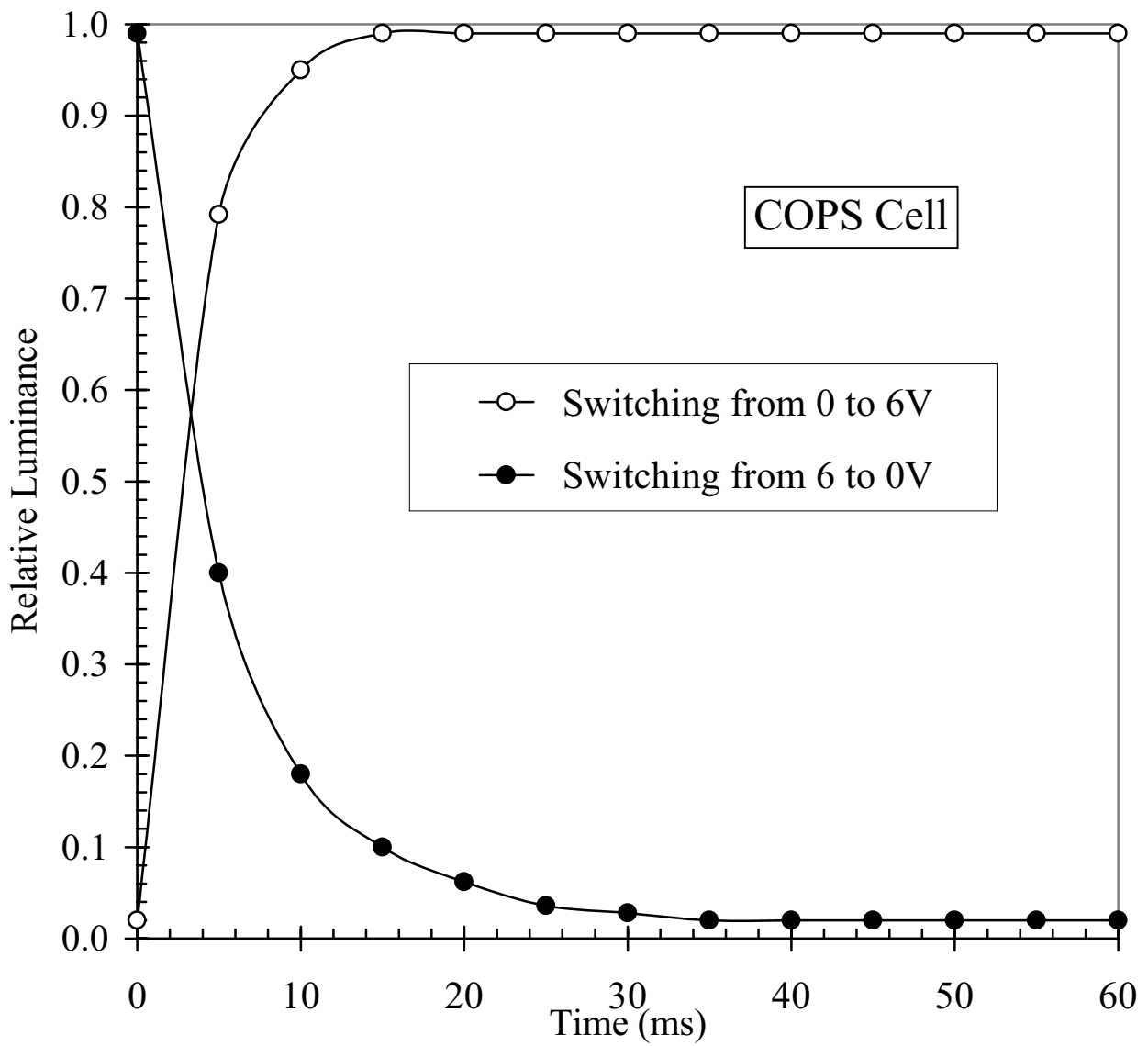


Figure 7.

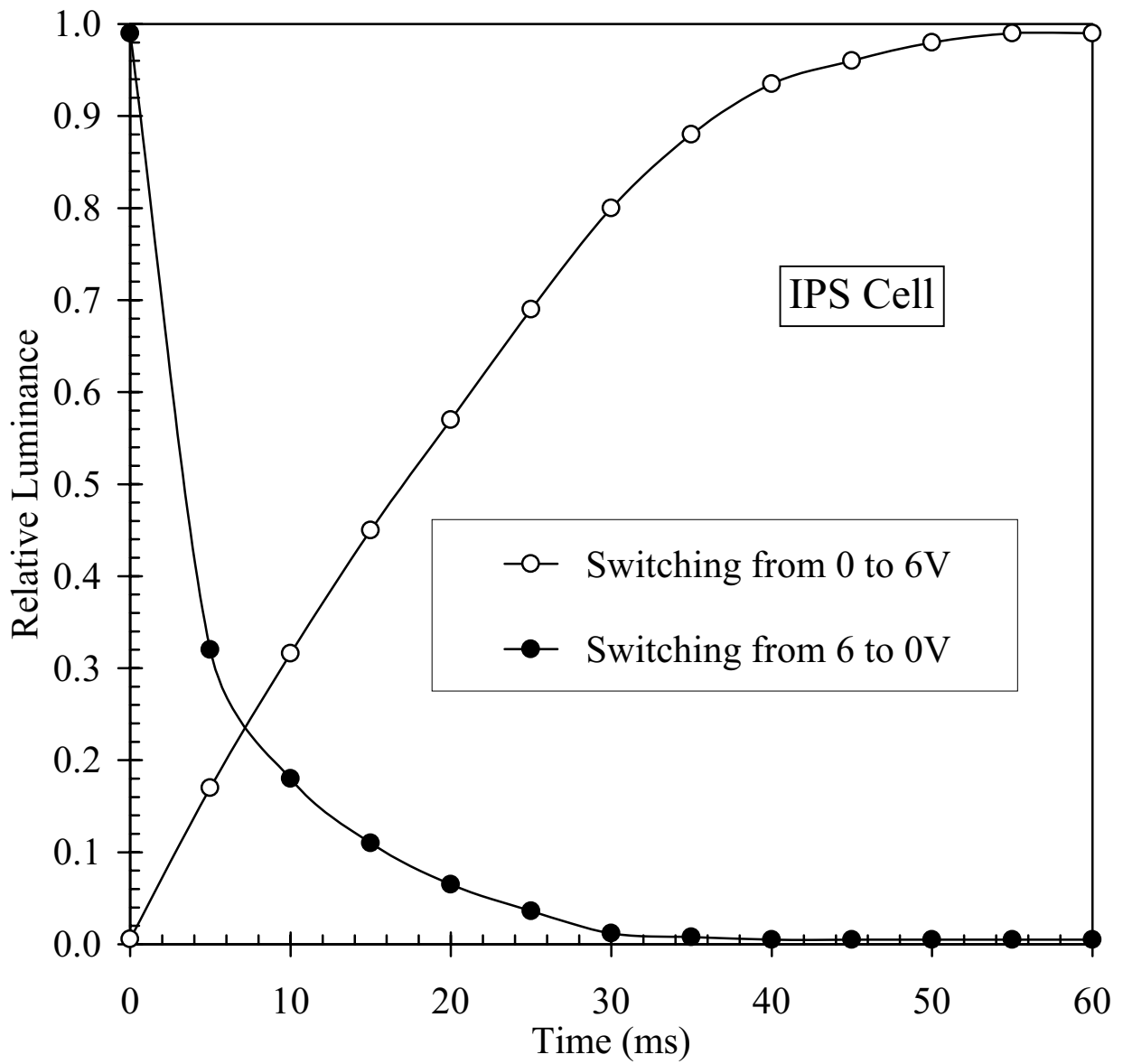


Figure 8.

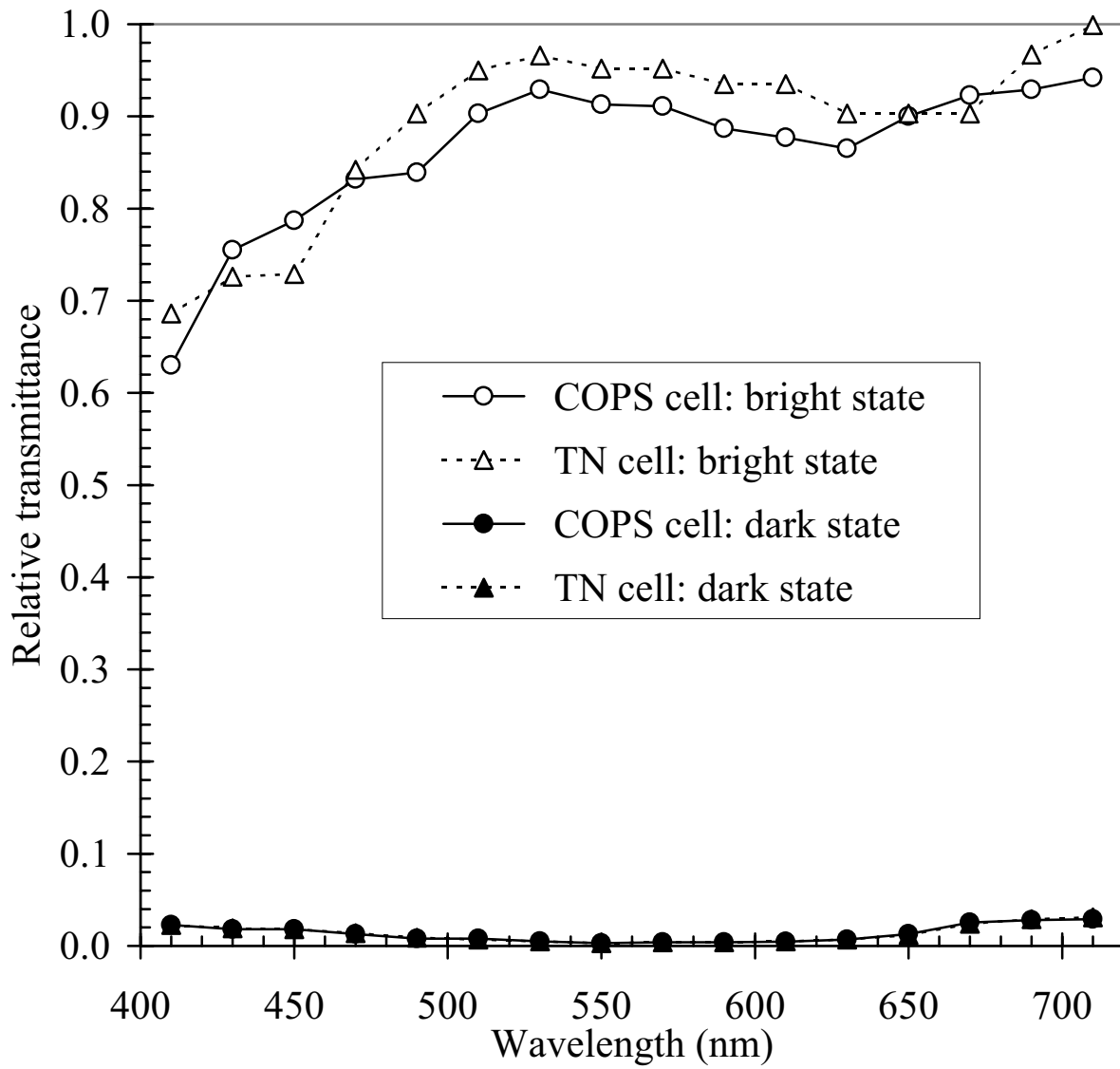


Figure 9.

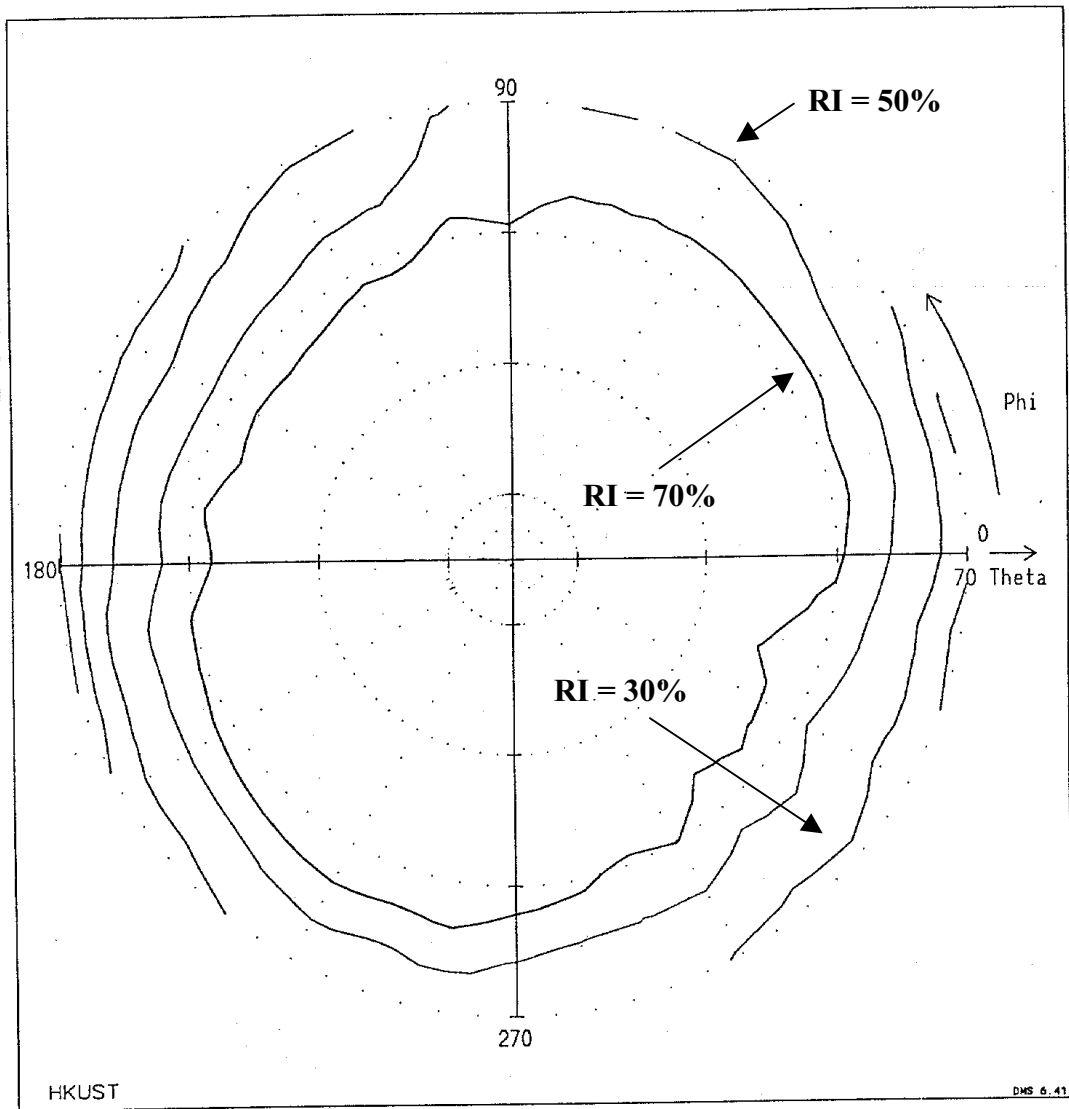


Figure 10.

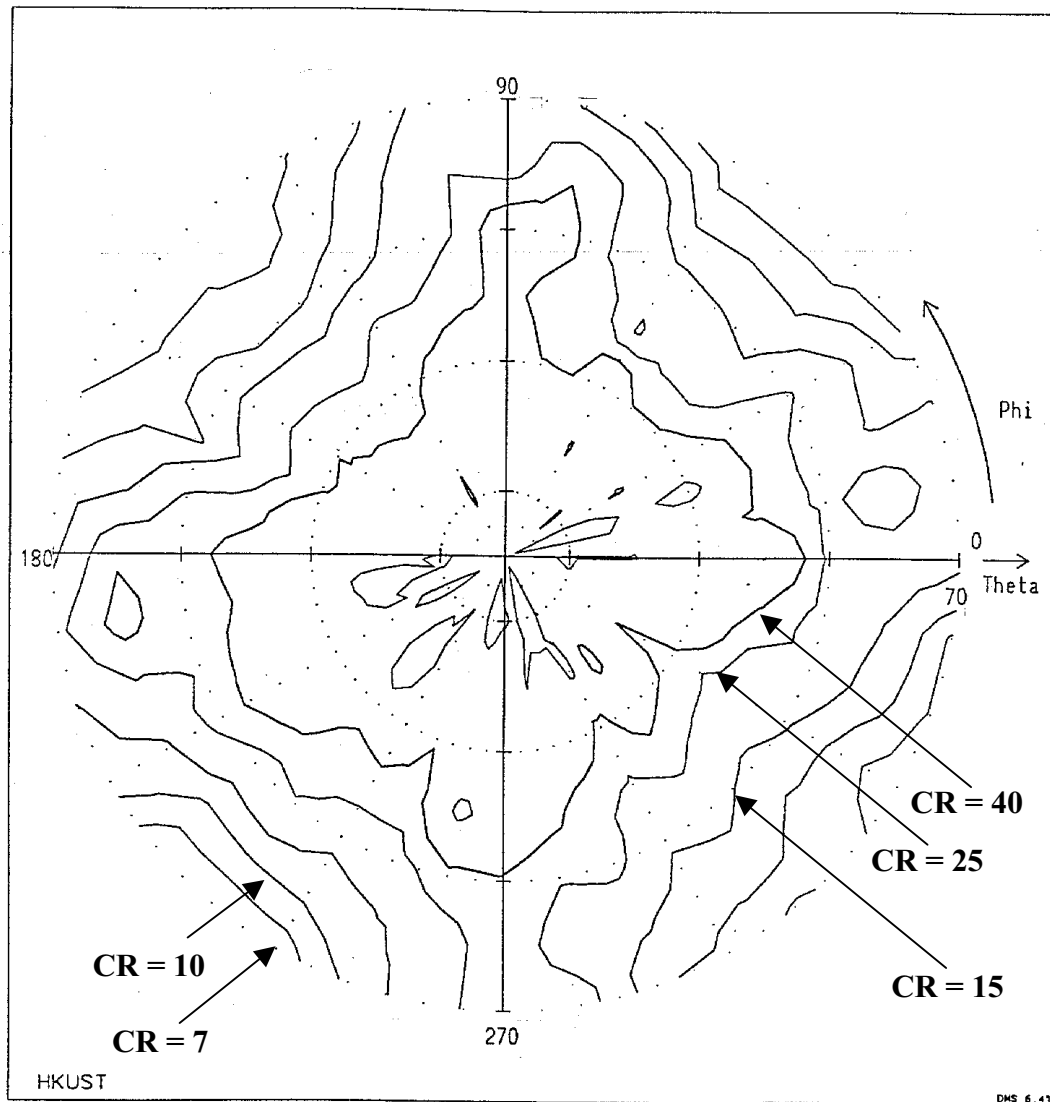


Figure 11.

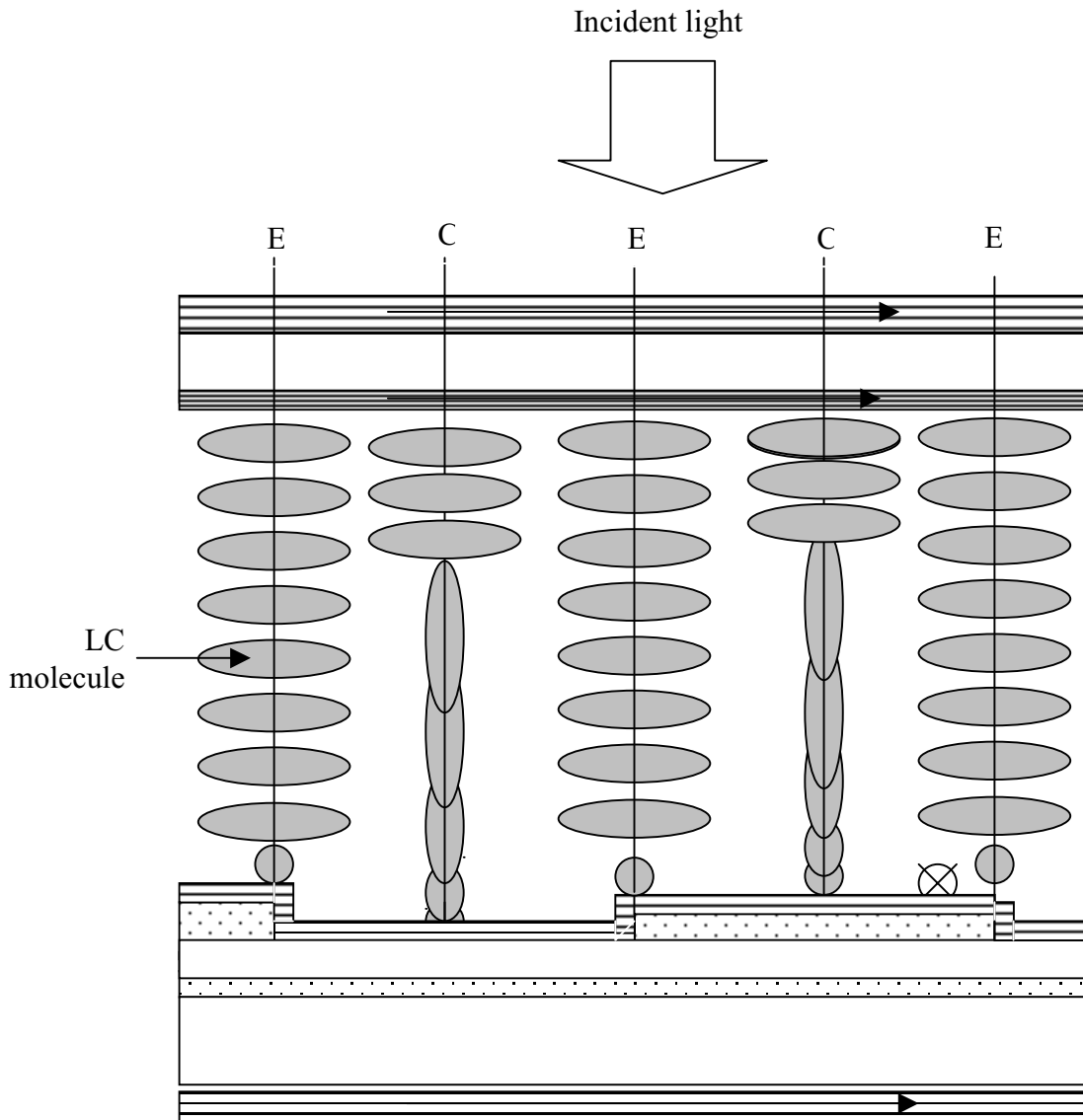


Figure 12.

